

# Spatial Filtering of High Order Harmonics by an OFI Plasma Amplifier

J.P. Goddet<sup>1</sup>, S. Sebban<sup>1</sup>, Ph. Zeitoun<sup>1</sup>, J. Gautier<sup>1</sup>, C. Valentin<sup>1</sup>, F. Tissandier<sup>1</sup>, T. Marchenko<sup>1</sup>, G. Lambert<sup>1</sup>, J. Nejd<sup>1</sup>, B. Cros<sup>2</sup>, G. Maynard<sup>2</sup>, B. Robillard<sup>2</sup>, T. Mocek<sup>3</sup>, M. Kozlová<sup>3</sup> and K. Jakubczak<sup>3</sup>

<sup>1</sup> Laboratoire d'Optique Appliquée, chemin de la hunière, 91128 Palaiseau

<sup>2</sup> LPGP, Université Paris-Sud, 91405 Orsay, France

<sup>3</sup> Institute of Physics, Department of X-Ray Lasers, Prague, Czech Republic

**Abstract.** It is now possible to produce a 10 Hz soft x-ray laser beam having very high optical qualities. The solution consists in seeding an optical-field-ionized population inverted plasma amplifier with the 25<sup>th</sup> harmonic of an infrared laser. This concept was successfully realized in LOA in 2004 and an extensive investigation of the source has been recently performed. Indeed we demonstrate the first diffraction-limited laser beam in the soft x-ray spectral range. This laser beam at a central wavelength of 32.8 nm, emitted with a divergence of 0.67 mrad at a repetition rate of 10 Hz. The beam exhibits a regular Gaussian spatial profile, and wavefront distortions smaller than  $\lambda/17$ . A theoretical analysis of these results shows that this high beam quality is due to spatial filtering of the seed beam by the plasma amplifier aperture.

## 1 Introduction

Until now, in all the soft x-ray laser (SXRL) schemes operating at saturation, population inversion between the levels of the lasing ion is induced by electron collisional excitation, leading to high gain value at short wavelength [1]. The short lifetime of the gain and the absence of high reflectivity soft x-ray optics, make the use of this SXRL amplifier in a complete laser cavity impossible. For this reason, SXRL emission generally results from the single-pass amplification of spontaneous emission. As a consequence, SXRL radiation is characterized by an inhomogeneous beam profile [2], a low spatial coherence [3] and important wavefront distortions [4], which limits the use of SXRL for applications that require a highly intense, coherent, soft x-ray photon flux in a sub-micron spot size. To fully explore the potential of plasma-based SXRL sources, improving their spatial beam quality is a crucial bottleneck to be overcome. A promising solution to be explored consists in seeding a soft x-ray plasma amplifier with a High Order Harmonic (HOH) seed beam [5]. This Seeded soft x-ray laser (SSXRL) approach is a direct analogy of the “oscillator-amplifier” concept commonly used for infrared (IR) laser system, applied

in the soft x-ray range. Here the HOH beam plays the role of an oscillator which is injected and amplified while propagating through a population-inverted SXRL plasma column. This emerging scheme [6-7] offers a prospect for compact SXRL chain combining both the high energy extracted from the plasma amplifier as well as the high optical quality of the HOH beam [8-9].

We report on the first observation of a diffraction-limited laser beam at 32.8 nm achieved by seeding an Optical Field Ionised (OFI) SXRL amplifier [10] with a HOH beam. The 32.8 nm SSXRL beam exhibits a circular energy distribution with a divergence of 0.67 mrad (half angular with at  $1/e^2$ ) Wavefront distortions were measured to be smaller than  $\lambda/17$  (1.9 nm). Numerical simulations show that the properties of the measured wavefront and energy distribution of the SSXRL result from spatial filtering of the seed beam in the amplifying plasma column.

## 2 Experimental setup

The experiment was performed at the Laboratoire d'Optique Appliquée (LOA) using a 10 Hz, multi-terawatt Ti:sapphire laser system providing two independent 34 fs laser beams at a central wavelength of 815 nm [11]. The first IR laser beam, containing about 10 mJ, was used to generate the HOH beam inside a 7 mm long gas cell filled with 30 mbar of Ar. The 25<sup>th</sup> harmonic of the IR laser was closely matched to the wavelength of the lasing transition of the SXRL amplifier. A grazing incidence toroidal mirror imaged the output of the HOH source with a magnification of 1.5 at the entrance of the amplifier cell. The second IR beam, circularly polarized, was delivering ~600 mJ on target. This pump beam, focused to a spot diameter of 38  $\mu\text{m}$  (at  $1/e^2$ ) inside a 7.5 mm long gas cell filled with Kr, was used to create the OFI amplifying plasma column which drives the  $3d^94d (1S^0) \rightarrow 3d^94p (1P^1)$  transition of the  $\text{Kr}^{8+}$  ion at 32.8 nm [12].

## 3 Far field pattern

The spatial energy distribution of the SSXRL and HOH beams were measured after reflection from a removable 45°, soft X-ray mirror made of  $\text{B}_4\text{C}/\text{Mo}/\text{Si}$  tri-layers, by a Charge Coupled Detector (CCD) camera. A 300 nm thin aluminium filter was used to block the IR beam. Figure 1(a) shows the energy distribution of the seed HOH. The HOH beam exhibits an astigmatic profile with horizontal and vertical divergence of 1.32 mrad and 0.48 mrad, respectively, due to a slight misalignment of the toroidal coupling mirror. This HOH beam is then injected into the 32.8nm amplifier, set for optimized parameters,

i.e. filling pressure of 20 mbar, and cell length of 7.5 mm. The energy distribution resulting from the amplification of the HOH beam into the plasma column is dramatically improved as shown in Fig. 1(b). The intense monochromatic radiation is emitted in the direction of the HOH beam, and has a divergence of  $0.67 \pm 0.07$  mrad ( $1/e^2$ ). The spatial beam distribution is nearly Gaussian. Note that such a high beam quality has never been observed for other plasma-based SXRLs. In general, SXRLs exhibit highly contrasted intensity modulations (or speckles) forming a complex and irregular pattern [13], which is a direct consequence of low spatial coherence combined with the high temporal coherence of the amplified spontaneous emission (ASE) radiation [2]. Here the amplification of the partially coherent HOH beam strongly enhances the spatial coherence and results in a smooth beam pattern.

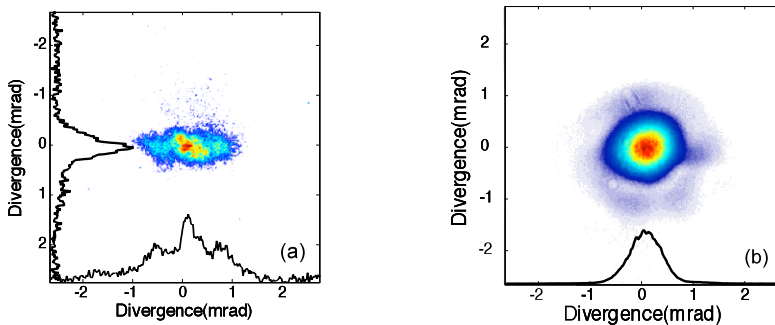


**Fig. 1** Spatial profile of (a) the HHG and (b) the SSXRL beams.

#### 4 Wavefront measurement

The wavefront of the SSXRL was measured with a soft x-ray Hartmann sensor [14]. In the Hartmann wavefront analysis a beam passes through a hole array and is projected onto a CCD camera that detects the beamlet sampled by each hole. The position of each individual spot centroid is measured and compared with a reference position. The Hartman technique allows energy and phase to be measured simultaneously. The soft x-ray Hartmann sensor was made of a 100 microns thick, nickel plate placed at about 20 cm in front of a back-illuminated XUV CCD. The Nickel plate contained a matrix of  $51 \times 51$  square holes ( $80 \mu\text{m} \times 80 \mu\text{m}$  and separated by  $380 \mu\text{m}$ ), over an area of  $15 \times 15 \text{ mm}^2$ . This diagnostic permits to reconstruct the wavefront with a resolution of  $\lambda/20$  at  $32.8 \text{ nm}$  [15]. A more accurate analysis of the spatial coherence can be obtained by combining intensity and phase measurements to get full information on the complex amplitude of the laser field. In the plane

of the Hartmann detector, the complex amplitude of the laser field can be written as

$$E_H(x, y, z = z_H) = \sqrt{I_{SXRL}(\theta_x, \theta_y)} \exp \left[ i \frac{\pi}{\lambda_{SXRL}} \left( \frac{x^2 + y^2}{z_H} + 2\delta(\theta_x, \theta_y) \right) \right] \quad (1)$$

In this equation,  $z_H$  is the distance between the detector and the entrance of the plasma,  $\theta_x = x/z_H$  and  $\theta_y = y/z_H$  are the beam divergences in the two directions perpendicular to the beam axis,  $I_{SXRL}$  is the laser intensity as reported in Fig. 1 and  $\delta(\theta_x, \theta_y)$  represents the fluctuation of the wavefront;  $\delta(\theta_x, \theta_y) = 0$  corresponds to a fully coherent, diffraction limited beam. Figure (2a) shows a typical example of the values of  $\delta(\theta_x, \theta_y)$  for the seed HOH beam, measured by the Hartmann sensor. The HOH beam exhibits large phase fluctuations, with an average distortion of about  $0.3 \times \lambda_{SXRL}$  root-mean-square (rms). The wavefront fluctuations in the case of the SSXRL beam are shown in Fig. 2b. In comparison to the HOH case (Fig. 2a), the amplitude of the wavefront fluctuations of the SSXRL are much smaller, with a rms value of only  $0.058 \times \lambda_{SXRL}$ , which corresponds to less than  $\lambda/17$  (1.9 nm). According to the Marechal criterion, which states that a system is regarded as well corrected if the wavefront distortion does not exceed  $\lambda/14$  [16], the generated SSXRL can be considered as a fully coherent diffraction-limited beam, which has never been demonstrated so far. Earlier works showed that neon-like Ar capillary discharge-driven SXRL at 46.9 nm exhibits wavefront distortion of  $3 \times \lambda_{SXRL}$ , which is, to our date, the only measurement performed for plasma-based SXRL source [17].

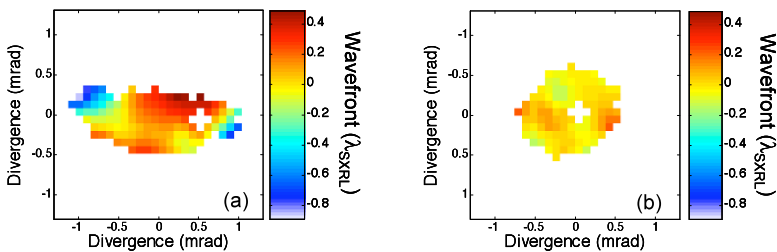


**Fig. 2** Measured wavefront of (a) the HHG beam, and. (b) the seeded EUV laser at 32.8 nm.

## 5 Reconstructed sources

A simple theoretical analysis of the spatial coupling of the seed HOH beam into the plasma amplifier allows understanding how such a high beam quality can be achieved. As the intensity and the phase of the beams were measured using the Hartman sensor, the values of the complex amplitude of the electric field, Eq. (1), are known in the plane of the detector at each small hole position. Using a  $\chi^2$  minimization fit, these values are projected on a HG basis (18), to make possible the reconstruction of the complex amplitude of either the HOH beam or the SSXRL one anywhere on the path of the beam.

The results of this analysis are presented in Figs 3. Figure 3(a) shows the HOH beam energy distribution reconstructed at the entrance of the amplifying plasma column, which is found to be oval with dimensions of  $55 \times 116 \mu\text{m}^2$  (at  $1/e^2$ ). The SSXRL energy distribution at the exit of the plasma is shown in Fig. 3b. It has a more symmetrical shape with a surface of  $58 \times 77 \mu\text{m}^2$  (at  $1/e^2$ ). These beam reconstructions indicate that, in terms of energy, the coupling between the HHG beam and the amplifier is well optimized as 60% of the incoming energy is amplified by the plasma. Thus the spatial filtering is quite efficient because the main part of the phase distortion comes from the outer part of the HHG beam.

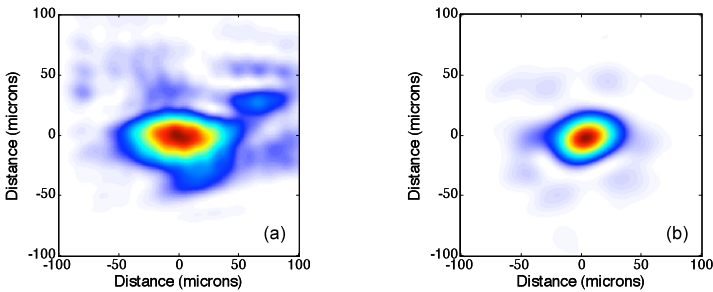


**Fig. 3** (a) Reconstructed profile of the HHG beam at the entrance of the amplifying plasma, and (b) reconstructed source size of the SSXRL beam.

## 6 Spatial filtering simulation

To analyze the importance of spatial filtering in the reduction of the wavefront distortions we used a simplified model in which the plasma is considered as a perfect amplifier, where the amplified output signal is a coherent reproduction of the input HOH beam. The plasma is assumed to be a cylinder of length  $L=7.5$  mm and of radius  $R$ . The value for the Rayleigh length of the HHG

beam is one order of magnitude larger than  $L$ , so that diffraction effect inside the plasma can be safely neglected. Therefore the complex amplitude for the SSXRL, at the exit of the plasma, takes the simple form

$$E_{SSXRL}(x, y, z = L) = \sqrt{G} E_H(x, y, z = 0) H\left(R - \sqrt{x^2 + y^2}\right), \quad (2)$$

Where  $G$  is the amplifying factor,  $H(u)$  is the heaviside step function and  $E_H$  is the complex amplitude defined in Eq. (1) for the HHG beam case. In Eq. (2), due to the large value of  $G$  and also to absorption by non-ionized gas, the amplitude of the field outside the plasma has been set to zero.

We see from Eq. (2) that, besides a constant factor, the influence of the plasma amplifier on the HHG beam is identical to the effect of a circular diaphragm.  $E_{SSXRL}(x, y, z = L)$  was determined from Eq. (4), and projected again on the HG basis, in order to determine the complex amplitude of  $E_{SSXRL}(x, y, z = z_H)$  in the plane of the Hartmann detector. These calculations were performed for plasma radius ranging from 15  $\mu\text{m}$  up to 1000  $\mu\text{m}$ . Figure 4 shows the distribution of energy as determined from  $E_{SSXRL}(x, y, z = z_H)$  for 4 values of the plasma radius a)  $R = 100 \mu\text{m}$ , b)  $R = 50$ , c)  $R = 30$  and d)  $R = 20 \mu\text{m}$ . As observed in Figure 4, the energy distribution of the SSXRL is strongly modified for plasma radius smaller than 100  $\mu\text{m}$ . For the larger radius Fig. 4.a, the HOH beam size at the entrance of the plasma (Fig. 3a) is smaller than the plasma size, and the amplified beam shape is not modified. By decreasing the plasma radius down to 25  $\mu\text{m}$ , the beam evolves from astigmatic to a perfect circular beam, as observed experimentally. For a plasma of 30  $\mu\text{m}$  (Fig. 4c), the divergence of the SSXRL beam is of  $0.46 \text{ mrad} \times 0.57 \text{ mrad}$ , in reasonable agreement with our experimental measurements 0.67 mrad (Fig. 1b). For a plasma radius smaller than 25  $\mu\text{m}$  (Fig. 4d), the divergence of the SSXRL beam increases due to diffraction.

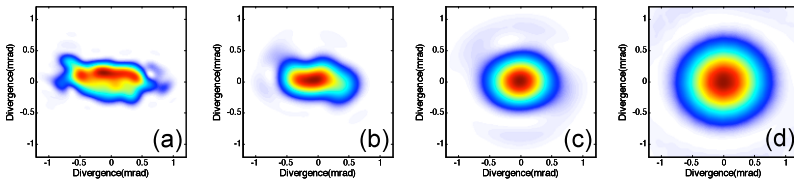


**Fig. 4** 2D reconstruction of the far-field pattern of the SSXRL beam by spatial filtering of the HHG beam through a plasma aperture with variable radius: (a) 100  $\mu\text{m}$ , (b) 50  $\mu\text{m}$ , (c) 30  $\mu\text{m}$ , (d) 20  $\mu\text{m}$ .

The variation of wavefront distortion as a function of the plasma radius is plotted in Fig. 5. It shows that for our experimental conditions, the wavefront distortions of the SSXRL beam are significantly reduced for a plasma radius smaller than  $60\ \mu\text{m}$  and that the diffraction limit ( $\lambda/14$ ) is reached when the amplifying plasma radius is smaller than  $37\ \mu\text{m}$ . According to these calculations our measurements of the wave front suggest that the HOH beam was filtered by a  $30\ \mu\text{m}$  radius plasma column; this value is in good agreement with the ones determined from the divergence of the beam and from the energy distribution (Fig. 3a). The agreement between experimental observations and this simple analysis implies that the plasma amplifier has a very low level of transverse dispersion, much lower than the dispersion of the intensity of the IR pump beam. This is due to the highly non-linear character of the OFI process, in which the lasing ion  $\text{Kr}^{8+}$  can be produced without significant changes of the plasma properties, while allowing nearly one order of magnitude variation for the IR intensity.

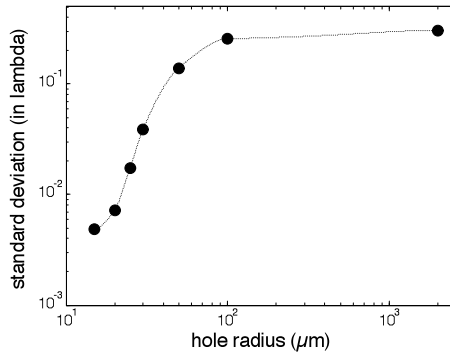


**Fig. 5** Calculated wavefront of the of the SSXRL beam as a function of the plasma radius.

## 7 Conclusion

In conclusion, by seeding a laser created plasma amplifier we have demonstrated that it is possible to generate an intense soft x-ray beam having all the optical properties of common visible/IR/UV lasers. Our measurements suggest that thanks to the perfect wavefront it should be possible to focus the SSXRL beam into a near diffraction-limited spot, and thus achieve a soft x-ray intensity close to  $10^{15}\ \text{W}\cdot\text{cm}^{-2}$ . In a near future we anticipate a significant improvement of this concept, e.g. by using waveguiding technique to increase the length of the amplifier and thus boost up the output energy by at least one order of magnitude [19]. The excellent spatial beam quality, coupled to a high

longitudinal coherence make this source an excellent scientific tool for applications such as soft x-ray holography, phase contrast imaging, and microscopy.

## References

1. H. Daido, *Rep. Prog. Phys.* 65, 1513 (2002)
2. S. Sebban et al., *JOSA B* 80, 195 (2003)
3. J. Ph. Goddet et al., *Opt. Lett.* 32, 1498 (2007)
4. J.J. Rocca et al., *Phys. Rev. Lett.* 73, 2192 (1994)
5. T. Ditmire et al., *Phys. Rev. A* 51, 0R4337 (1995)
6. Ph. Zeitoun et al., *Nature* 431, 466 (2004)
7. Y. Wang et al., *Phys. Rev. Lett.* 97, 123901 (2006)
8. L. Le Déroff et al., *Phys. Rev. A* 61, 043802 (2000)
9. K. Midorikawa et al., *Phys. Rev. A* 66, 021802(R) (2002)
10. B. E. Lemoff et al., *Optics Letters* 19: 569-571 (1994)
11. M. Pittman et al., *Appl. Phys. B* 74, 529 (2002).
12. S. Sebban et al., *Phys. Rev. Lett.* 89 253901-1 (2002)
13. S. Sebban et al., *JOSA B* 80, 195 (2003)
14. P. Mercere et al. *Opt. Lett.* Vol. 28 (2003) 1534
15. W.H. Southwell, *J. Opt. Soc. Am.* 70, 998 (1980)
16. A. Marechal, *Rev. D'Optique*, 26, 257 (1947)
17. S. Le Pape et al., *Phys. Rev. Lett.* 88, 183901-1 (2002)
18. A.E. Siegman *Lasers*, University Science Books, Sausalito, California (1986)
19. B. Cros et al., *Phys. Rev. A* 73, 033801 (2006)